Title
Robustness and sensitivities of central U.S. summer convection in the super-parameterized CAM: Multi-model intercomparison with a new regional EOF index

Journal
Geophysical Research Letters, 40(12)

ISSN
0094-8276

Authors
Kooperman, Gabriel J
Pritchard, Michael S
Somerville, Richard CJ

Publication Date
2013-06-28

DOI
10.1002/grl.50597

Robustness and sensitivities of central U.S. summer convection in the super-parameterized CAM: Multi-model intercomparison with a new regional EOF index

Gabriel J. Kooperman,[1] Michael S. Pritchard,[2] and Richard C. J. Somerville[1]

Received 22 April 2013; revised 24 May 2013; accepted 29 May 2013; published 18 June 2013.

[1] Mesoscale convective systems (MCSs) can bring up to 60% of summer rainfall to the central United States but are not simulated by most global climate models. In this study, a new empirical orthogonal function based index is developed to isolate the MCS activity, similar to that developed by Wheeler and Hendon (2004) for the Madden-Julian Oscillation. The index is applied to compactly compare three conventional- and super-parameterized (SP) versions (3.0, 3.5, and 5.0) of the National Center for Atmospheric Research Community Atmosphere Model (CAM). Results show that nocturnal, eastward propagating convection is a robust effect of super-parameterization but is sensitive to its specific implementation. MCS composites based on the index show that in SP-CAM3.5, convective MCS anomalies are unrealistically large scale and concentrated, while surface precipitation is too weak. These aspects of the MCS signal are improved in the latest version (SP-CAM5.0), which uses high-order microphysics. **Citation:** Kooperman, G. J., M. S. Pritchard, and R. C. J. Somerville (2013), Robustness and sensitivities of central U.S. summer convection in the super-parameterized CAM: Multi-model intercomparison with a new regional EOF index, *Geophys. Res. Lett.*, *40*, 3287–3291, doi:10.1002/grl.50597.

1. Introduction

[2] Organized propagating storms, or mesoscale convective systems (MCSs), bring up to 60% of summer rainfall to the central U.S., which water this sensitive agricultural region [*Carbone and Tuttle*, 2008]. Changes in the patterns and intensity of rainfall associated with these storms can lead to devastating drought conditions at one end of the spectrum and severe flood damage at the other. To understand how MCS activity may respond to climate change, a realistic representation of the physical mechanisms that generate MCSs in nature is needed in models that also capture the global-scale physics of climate change.

[3] Unfortunately, most conventional global climate models (GCMs) are unable to simulate mid-latitude MCSs and disagree on the sign of future precipitation trends in the central U.S. [*Lee et al.*, 2007; *Solomon et al.*, 2007]. Representing the mesoscale in GCMs is difficult because the relevant physics straddle the divide between parameterized and resolved scales [*Moncrieff*, 1992]. Other issues include poorly resolved topography and convective parameterization too closely locked to the solar insolation cycle.

[4] The first evidence of a promising MCS signal in a climate change capable GCM has recently been documented in an intermediary development version of the super-parameterized (SP) Community Atmosphere Model (CAM) (SP-CAM, version 3.5). In SP-CAM3.5, *Pritchard et al.* [2011] identified nocturnal eastward propagating convection in the central U.S. with realistic MCS propagation speed and relative flow dynamics. This SP MCS signal is scientifically interesting for two reasons. First, if it is shown to be a valid analog to nature, it may provide a path to reliable climate change predictions in the central U.S. Second, it adds to the debate about what physics govern MCS propagation.

[5] Observations and cloud-resolving models (CRM) indicate that both large- and small-scale physics are involved in the organization and propagation of MCSs in nature. Propagation mechanisms include horizontal advection of potential vorticity anomalies [*Li and Smith*, 2010], the veering of the low-level jet moisture convergence zone [*Trier et al.*, 2006], and small-scale cold pool density currents [*Carbone et al.*, 2002]. The relative importance of each scale regime can be hard to disentangle in data or mesoscale models. However, in SP-CAM, only large-scale processes have a long-range effect due to the use of laterally periodic CRM arrays. Thus, a realistic MCS in SP-CAM argues against the criticality of small-scale processes in mediating MCS propagation.

[6] To date, the MCS signal has only been qualitatively assessed in a single version of SP-CAM. The signal in SP-CAM3.5 was apparent in atmospheric heating but was absent in surface precipitation. Is MCS activity a robust effect of SP or a fluke of one model version? Do simulated storms compare to the observed areal extent, magnitude of precipitation and liquid/ice condensate, and frequency of occurrence? Is SP critical, or can modern versions of the conventionally parameterized CAM capture the signal?

[7] To answer these questions, a new regional MCS index has been developed based on empirical orthogonal functions (EOFs), similar to the *Wheeler and Hendon* [2004] Madden-Julian Oscillation (MJO) index. Following this method, the angular relationship between principle component (PC) time series defines an index that denotes the strength, phase, and location of maximum convection.

Additional supporting information may be found in the version of this article.

[1]Scripps Institution of Oceanography, University of California, San Diego, La Jolla, California, USA.
[2]Department of Atmospheric Sciences, University of Washington, Seattle, Washington, USA.

Corresponding author: G. J. Kooperman, Scripps Institution of Oceanography, University of California, San Diego, 9500 Gilman Dr., Dept. 0224, La Jolla, CA 92093-0224, USA. (gkooperman@ucsd.edu)

0094-8276/13/10.1002/grl.50597

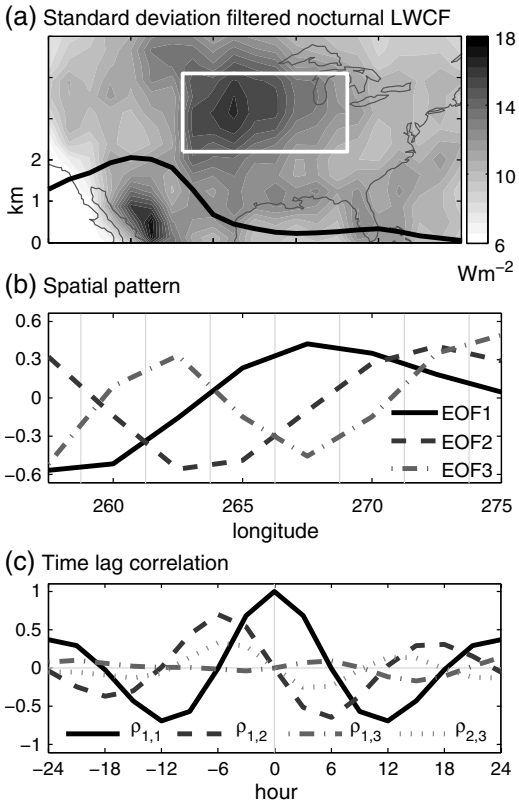

Figure 1. (a) Standard deviation of 12 to 48 h band-pass filtered nocturnal (00–06 CST) longwave cloud forcing (W/m^2); the black line is the average topography from 36° to 45° latitude, and the white box is the EOF analysis region. (b) Spatial patterns of EOFs. (c) Time-lag correlations between PC time series.

This new index is applied to quantitatively compare the statistics of existence, frequency, and composite MCS structure in observations and several conventional- and super-parameterized versions of CAM.

2. Observations and Models

2.1. Observations

[8] The MCS index was developed using 23 years (1984–2006) of May, June, July, and August (MJJA) longwave cloud forcing (LWCF) from the NASA Global Energy and Water Cycle Experiment, Surface Radiation Budget (SRB) version 3.1 [*Stackhouse et al*., 2011]. SRB provides 1° resolution, three-hourly, top-of-the-atmosphere instantaneous fluxes. SRB is a combined product of satellite observations, reanalysis data, and a radiative transfer model that has been evaluated against direct satellite and ground-based observations [*Allan*, 2011; *Stackhouse et al*., 2011; *Zhang et al*., 2013].

[9] Composite precipitation statistics based on index-phase criteria are also compared between observations and models. Hourly accumulated precipitation from the National Centers for Environmental Prediction Climate Prediction Center (CPC) is based on rain gauge data objectively analyzed to a 2° by 2.5° grid [*Higgins et al*., 1996]. The CPC composite has been used to analyze the representation of precipitation in several reanalysis models and diurnal summer precipitation over the U.S. [*Bukovsky and Karoly*, 2007; *Higgins et al*., 1997].

2.2. Community Atmosphere Model

[10] Two official releases (3.0 and 5.0) and one development (3.5) version of the National Center for Atmospheric Research (NCAR) CAM were run as stand-alone atmospheric GCMs for this study. All used present-day sea surface temperatures and sea ice, and an interactive land surface. The dynamical core was semi-Lagrangian in CAM3.0 at a standard spectral resolution of T42 (~250 km at 36°N) with 26 vertical levels and was finite volume in CAM3.5 and CAM5.0 at a standard resolution of 1.9° by 2.5° (~225 km at 36°N) and 30 vertical levels. Parameterized physics has developed significantly from versions 3.0 and 3.5 to 5.0, including the addition of two-moment cloud microphysics, vertical entrainment and momentum transport in the deep convection scheme, moist turbulence in the shallow convection scheme, and aerosol interactions with the microphysical and radiative transfer schemes. Two-moment microphysics based on *Morrison and Gettelman* [2008] was developed from earlier CRM schemes and improves both shallow and deep precipitation regimes (for details, see *Collins et al*. [2004] for 3.0, *Neale et al*. [2008] for 3.5, and *Neale et al*. [2010] for 5.0).

2.3. Super-Parameterization

[11] *Khairoutdinov and Randall* [2001] implemented SP in CAM3.0 by embedding two-dimensional CRMs in each grid column of CAM to explicitly simulate cloud-scale processes rather than rely on statistical parameterization. CAM supplies each embedded CRM with a large-scale forcing, and the CRM returns a convective tendency [*Grabowski and Smolarkiewicz*, 1999]. Recently updated by *Wang et al*. [2011], the CRM in SP-CAM5.0 includes aerosol-radiation/cloud interactions and two-moment microphysics. All versions of SP-CAM have the same outer configuration as their CAM counterparts and CRM levels colocated with CAM. The CRM resolutions, horizontal domain sizes, and orientations were 4 km, 1×32, and east-west in 3.0; 1 km, 1×64, and east-west in 3.5; and 4 km, 1×32, and north-south in 5.0 following configurations described in *Khairoutdinov and Randall* [2001], *Pritchard et al*. [2011], and *Wang et al*. [2011], respectively.

3. Filtering and EOF Method

[12] An EOF-pair based index has been developed for evaluating central U.S. MCSs following techniques that have proven useful for compactly assessing quasi-periodic, pulse-like, intermittent convection on larger space and time scales [*Wheeler and Hendon*, 2004]. As pre-processing, all observational and model data were interpolated to a 1.9° by 2.5° grid (native to (SP)-CAM versions 3.5 and 5.0) and averaged to three-hourly time resolution. The MCS index was computed from three-hourly SRB LWCF from 23 boreal summers, band-pass filtered for 12 to 48 h timescales using a Lanczos digital filter. LWCF was deemed more suitable than outgoing longwave radiation, which has a strong diurnal temperature component.

[13] The nocturnal (00–06 CST) variance of the filtered signal shown in Figure 1a clearly delineates the well-known MCS activity zone in the central U.S. [*Anderson and Arritt*,

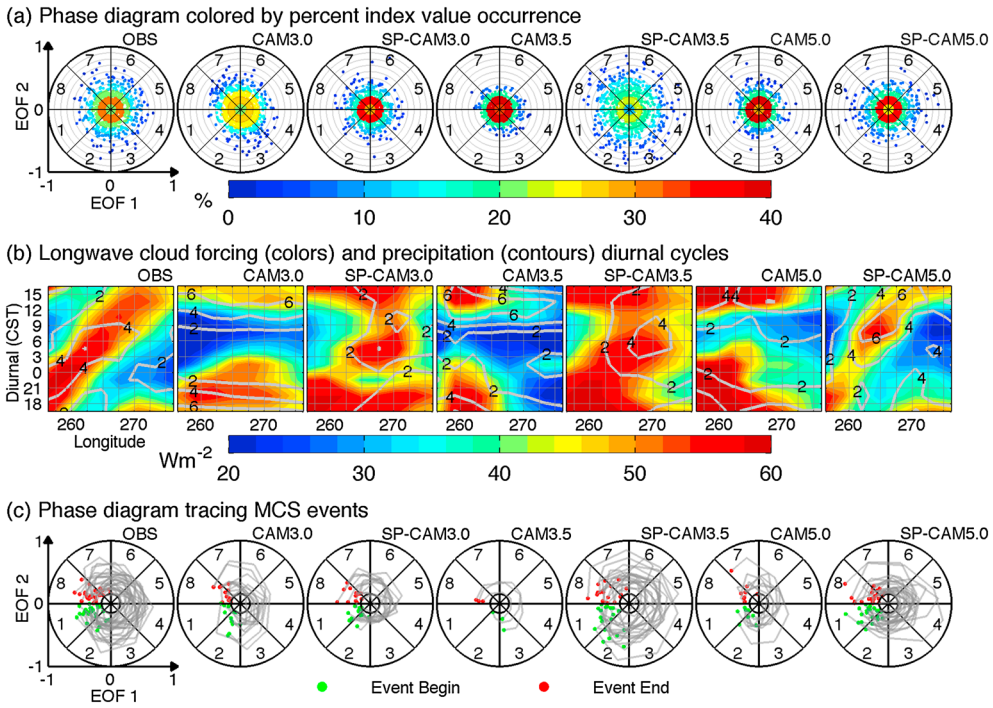

Figure 2. (a) Phase diagram of EOF PC time series 1 and 2 colored by percent index value occurrence in radial increments of 0.1 across all phases. (b) Longwave cloud forcing (colors, W/m^2) and precipitation (contours, mm/d) diurnal cycles for index values greater than 0.25. (c) Phase diagram of EOF PC time series 1 and 2 tracing MCS events based on event selection criteria explained in text, for observations and models.

1998]. The white box encloses the analysis region from 256° to 276° longitude and 36° to 45° latitude, extending from the eastern slope of the Rocky Mountains across the Great Plains. In this domain, 12 to 48 h filtered signals traveling through 75% of the zonal extent (~1300 km) correspond with zonal phase speeds roughly between 7 and 30 m/s, which is the radar-based estimated range of MCS travel rates [*Carbone et al.*, 2002].

[14] EOF analysis was applied on anomalies of meridionally averaged LWCF in this region after removing the background spatial mean at each time, which successfully targets the MCS signal of interest. The leading EOF-pair explains approximately 65% of the filtered variance with 35% and 30% from the first (EOF1) and second (EOF2) members, respectively (17% for EOF3). EOFs 1 and 2 have spatial patterns in zonal phase quadrature relationship over most of the domain and the highest time-lag correlation, peaking at a lag of −6 h. Taken together, these attributes represent the expected eastward propagating signal where EOF2 leads EOF1 by 6 h and ~430 km.

[15] Three-hourly LWCF from each model for a single summer was pre-processed as in the observations. The SP models reproduce native EOF pairs similar to SRB (supporting information), but all models were regressed onto the observed spatial patterns for EOFs 1 and 2 for consistency. The "MCS index" amplitude and angular phase come from collapsing the time series into polar coordinates, as is the convention in MJO analysis [*Wheeler and Hendon*, 2004]. Amplitudes were normalized by the maximum observed. Eight discrete phases are defined with an angular width of π/4 starting with phase 1 located near −π (at the west) with travel to the east (+π) corresponding to counterclockwise rotation.

4. Results and Discussion

[16] Joint histograms of the MCS index amplitude and phase relationship for models and SRB are depicted in Figure 2a for a single MJJA season. The highest percentages of amplitude values occur consistently between 0.1 and 0.2. The MCS signal is weakest in CAM3.5 and CAM5.0, which have less than 50 (25)% of values greater than 0.15 (0.25), relative to 64 (38)% in the observations. From the amplitude PDF view, CAM3.0 appears to be in the best agreement with 64 (39)%, followed by SP-CAM5.0 with 56 (29)%, SP-CAM3.0 with 52 (26)%, and SP-CAM3.5 with 76 (56)%. SP-CAM3.5 has the strongest signal with 17% of occurrences greater than 0.5, followed by SRB with 6%. SRB and all versions of SP-CAM have high amplitudes, with at least one value greater than 0.8.

[17] Unfiltered LWCF and precipitation composited above an index threshold of 0.25 and binned by local diurnal time in Figure 2b suggest that nocturnal convection is a robust effect of SP. An eastward slanted maximum across the observed domain shows the well-known nocturnal eastward MCS propagation. All versions of SP-CAM capture this nocturnal feature to some extent, which is not seen in any versions of CAM. SP-CAM5.0 has the best agreement with the observed width and colocated precipitation but under-simulates LWCF. SP-CAM3.5 over-simulates the magnitude and width of LWCF. Despite having realistic index amplitudes, CAM3.0 does not capture nocturnal activity.

[18] Several features in the observed panels of Figures 2a and 2b suggest a set of objective criteria for isolating MCS events based on an index amplitude threshold, duration, distance, and diurnal timing. Combined with the known span (500 to 2000 km) and duration (10 to 60 h) of MCS events

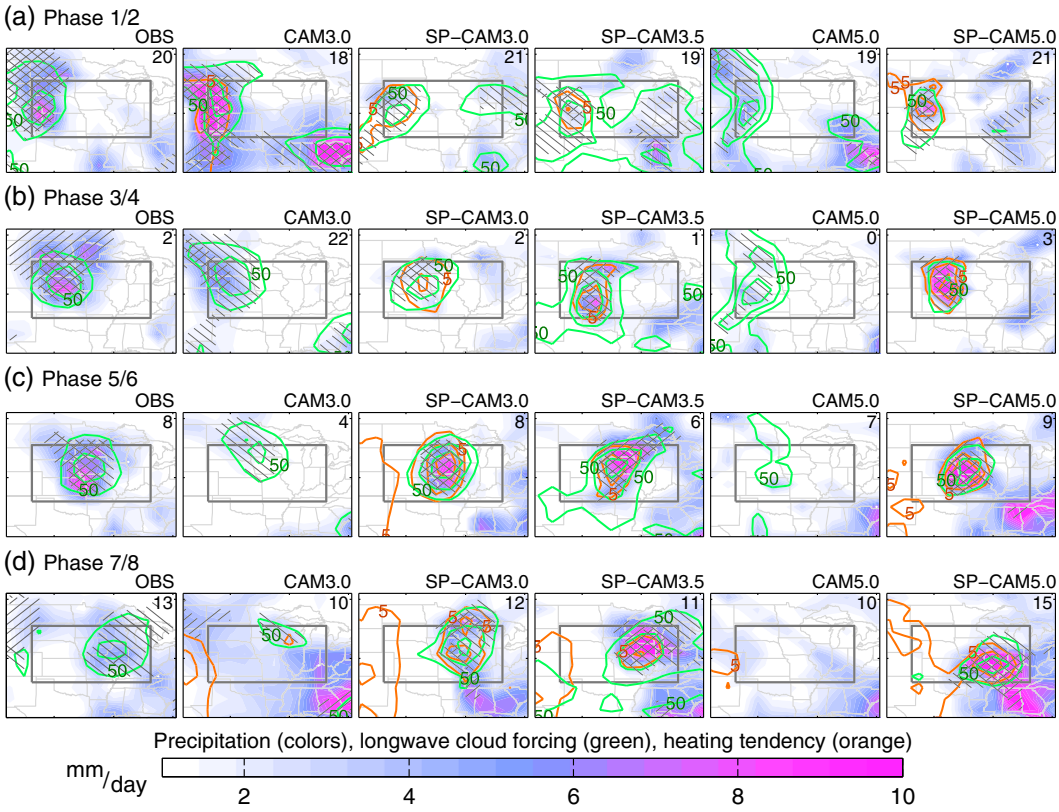

Figure 3. Composite event phase average of precipitation (colors, mm/d), longwave cloud forcing (green, increments of 25 W/m^2), and vertical standard deviation of model heating tendency (orange, increments of 2.5 K/d) for phases (a) 1 and 2, (b) 3 and 4, (c) 5 and 6, and (d) 7 and 8 in observations and models; right/45° (left/−45°) slashes indicate that precipitation (longwave cloud forcing) is significant at 95% confidence interval, the gray box is the EOF analysis region, and the numbers are the mean local diurnal time (CST).

reported by *Carbone et al*. [2002], this leads to the following event selection criteria: (1) at least three (9 h) consecutive index amplitudes greater than 0.15 propagating forward (east) in phase space, (2) spanning at least 70% of the domain (~1200 km), and (3) starting between 18 and 03 CST. The first criterion determines when high cloud continuously moves east, and the additional criterion helps to discriminate active nocturnal convection from clouds that are simply advected with the wind.

[19] SRB, SP-CAM3.5, and SP-CAM5.0 produce significantly more events than any other model. The above criteria identified an annual average and standard deviation of 24 ± 8 events in SRB; 13, 20, and 22 in SP-CAM; and 12, 3, and 9 in CAM for versions 3.0, 3.5, and 5.0, respectively. Although the number of events identified is sensitive to the specific threshold values chosen, the general result is robust across a range of choices. When the amplitude was restricted to values greater than 0.25, 12 events were identified in SRB, 14 in SP-CAM3.5, 10 in SP-CAM5.0, and not more than four in any other model.

[20] Objectively identified MCS events traced out in phase space are shown in Figure 2c. Observed event initiation strongly clusters in phase 1 and terminates in phase 8, with high amplitude values traced throughout. The best agreement with observations is seen in high amplitude values in SP-CAM3.5 and distance spanned in SP-CAM5.0.

[21] To assess the quality of simulated storms, event composites of precipitation and LWCF are depicted in Figure 3 for observations and all models, except CAM3.5, which had too few events to analyze. Each composite is an average of all times an event phase occurs, weighted by the amplitude value. Significance is determined at 95% confidence relative to 1000 randomly sampled averages having the same size as the composite. As a proxy for convective heating, the vertical standard deviation of free tropospheric heating (850 to 250 mb) from the physics package is also shown for models, as in *Pritchard et al*. [2011].

[22] In the observations and all versions of SP-CAM, statistically significant LWCF anomalies travel east with increasing phase. The signal in CAM3.0 appears to be a remnant of afternoon convection that diminishes with increasing phase and shows no active signal in the heating tendency or precipitation. LWCF in CAM5.0 is limited to half of the domain and does not represent propagation. Figure 3 provides further evidence that propagating nocturnal convection is a robust effect of SP and that SP-CAM5.0 is capturing it most realistically. Strong convective heating anomalies overlapping LWCF are detected in all versions of SP-CAM. Surface precipitation colocated with LWCF in the observations is also seen in SP-CAM5.0 and in some phases of SP-CAM3.0 and SP-CAM3.5.

[23] Although all versions of SP-CAM show MCS activity, distortions of the observed signal are evident. SP-CAM3.0 and SP-CAM3.5 under-simulate surface precipitation in phases 1 through 4 and over-simulate it in phases 7 and 8. The LWCF anomalies in these models are larger and broader

than observed, as a result of unrealistically large-scale and concentrated cloud ice. The timing of precipitation improves in SP-CAM5.0, coincident with more realistic LWCF values. SP-CAM5.0 has a tighter areal structure of LWCF in agreement with observations. A remaining deficiency in SP-CAM5.0 is visible in phases 7/8 where composite precipitation persists for too long and propagates too far. Offline tests (not shown) varying the event section criteria thresholds, with and without weighted composites, verify that these conclusions are robust.

[24] It is noteworthy that SP-CAM5.0 improvements include both reducing LWCF and increasing precipitation. This implies that the result is more than just a decrease in convective activity, which would impact both LWCF and precipitation in a similar manner. It may be an improvement in the partitioning between liquid and ice and suspended and falling condensate that resulted from the CRM update to two-moment microphysics by *Wang et al*. [2011]. Further work is needed to clarify this encouraging result.

5. Conclusions

[25] Mesoscale convection in the central U.S. is not simulated in conventional versions of CAM but is known to exist in one super-parameterized version. Analysis here shows it is furthermore a robust effect of SP spanning several versions. The strength of observed and simulated MCS activity is assessed using a new EOF index based on filtered regional LWCF. This index provides an efficient metric to isolate strong eastward propagating convection and, together with a simple set of criteria, identify MCS events and composite their propagation by phase. The newest version of SP-CAM5.0 is shown to have the best representation of composite MCS events. The magnitude and spatial extent of LWCF is in better agreement with observations, as is the colocated timing of surface precipitation.

[26] Future work will apply this MCS index to study mechanisms responsible for the improvement in SP-CAM5.0. What physics introduced by super-parameterization (i.e., sub-grid scale wind shear, memory, and non-CAPE-based convection) favor MCS development and propagation? Based on its demonstrated utility as a compact evaluation metric, sensitivity tests examining the index-composite structure of MCS dynamics, convective heating, moisture transport, and microphysics may provide some answers. Furthermore, realistically simulated convection in a GCM that also includes greenhouse gases and aerosols may enable research on how U.S. precipitation will respond to climate change.

[27] **Acknowledgments.** This study was supported by CMMAP (www.cmmap.org), a NSF STC (ATM-0425247), through sub-awards to R. Somerville and J. Helly, and by the DOE BER grant DE-SC0000658. M. Pritchard was supported by a NOAA Climate and Global Change Postdoctoral Fellowship. The NSF XSEDE provided computing resources on Kraken and Steele (TG-ATM090002 and TG-ATM100027). CAM development was led by the NCAR and supported by the NSF and the DOE. The authors are grateful to H. Morrison, M. Khairoutdinov, and M. Wang for SP-CAM development and simulations. SRB was provided by NASA LaRC ASDC GEWEX SRB. CPC was provided by NOAA/OAR/ESRL PSD. The authors also thank the reviewers.

[28] The Editor thanks Richard Carbone and an anonymous reviewer for their assistance in evaluating this paper.

References

Allan, R. P. (2011), Combining satellite data and models to estimate cloud radiative effect at the surface and in the atmosphere, *Meteorol. Appl.*, *18*, 324–333.

Anderson, C. J., and R. W. Arritt (1998), Mesoscale convective complexes and persistent elongated convective systems over the United States during 1992 and 1993, *Mon. Weather Rev.*, *126*, 578–599.

Bukovsky, M. S., and D. J. Karoly (2007), A brief evaluation of precipitation from the North American regional reanalysis, *J. Hydrometeorol.*, *8*, 837–846.

Carbone, R. E., J. D. Tuttle, D. A. Ahijevych, and S. B. Trier (2002), Inferences of predictability associated with warm season precipitation episodes, *J. Atmos. Sci.*, *59*(13), 2033–2056.

Carbone, R. E., and J. D. Tuttle (2008), Rainfall occurrence in the US warm season: The diurnal cycle, *J. Clim.*, *21*(16), 4132–4146.

Collins, W. D., et al. (2004), NCAR technical note: Description of the NCAR Community Atmosphere Model (CAM 3.0), Natl. Cent. for Atmos. Res., Boulder, Colo.

Grabowski, W. W., and P. K. Smolarkiewicz (1999), CRCP: A cloud resolving convection parameterization for modeling the tropical convecting atmosphere, *Physica D*, *133*(1–4), 171–178.

Higgins, R. W., J. E. Janowiak, and Y.-P. Yao (1996), A gridded hourly precipitation data base for the United States (1963–1993), NCEP/Climate Prediction Center Atlas 1, 46 pp., Natl. Cent. for Environ. Predict., College Park, Md.

Higgins, R. W., Y. Yao, E. S. Yarosh, J. E. Janowiak, and K. C. Mo (1997), Influence of the Great Plains low-level jet on summertime precipitation and moisture transport over the central United States, *J. Clim.*, *10*, 481–507.

Khairoutdinov, M. F., and D. A. Randall (2001), A cloud resolving model as a cloud parameterization in the NCAR Community Climate System Model: Preliminary results, *Geophys. Res. Lett.*, *28*(18), 3617–3620.

Lee, M.-I., et al. (2007), An analysis of the warm-season diurnal cycle over the continental United States and northern Mexico in general circulation models, *J. Hydrometeorol.*, *8*(3), 344–366.

Li, Y., and R. B. Smith (2010), The detection and significance of diurnal pressure and potential vorticity anomalies east of the Rockies, *J. Atmos. Sci.*, *67*(9), 2734–2751.

Moncrieff, M. W. (1992), Organized convective systems: Archetypal dynamic-models, mass and momentum flux theory, and parametrization, *Q. J. R. Meteorol. Soc.*, *118*(507), 819–850.

Morrison, H., and A. Gettelman (2008), A new two-moment bulk stratiform cloud microphysics scheme in the Community Atmosphere Model, version 3 (CAM3). Part I: Description and tests, *J. Clim.*, *21*, 3642–3659.

Neale, R. B., J. H. Richter, and M. Jochum (2008), The impact of convection on ENSO: From a delayed oscillator to a series of events, *J. Clim.*, *21*, 5904–5924.

Neale, R. B., et al. (2010), NCAR technical note: Description of the NCAR Community Atmosphere Model (CAM 5.0), Natl. Cent. for Atmos. Res., Boulder, Colo.

Pritchard, M. S., M. W. Moncrieff, and R. C. J. Somerville (2011), Orogenic propagating precipitation systems over the United States in a global climate model with embedded explicit convection, *J. Atmos. Sci.*, *68*(8), 1821–1840.

Solomon, S., D. Qin, M. Manning, Z. Chen, M. Marquis, K. B. Averyt, M. Tignor, and H. L. Miller (Eds.) (2007), *Climate Change 2007: The Physical Science Basis*, 996 pp., Cambridge Univ. Press, Cambridge, U. K.

Stackhouse, P. W. Jr., S. K. Gupta, S. J. Cox, T. Zhang, J. C. Mikovitz, and L. M. Hinkelman (2011), 24.5-year SRB data set released, *GEWEX News*, *21*(1), 10–12.

Trier, S. B., C. A. Davis, D. A. Ahijevych, M. L. Weisman, and G. H. Bryan (2006), Mechanisms supporting long-lived episodes of propagating nocturnal convection within a 7-day WRF model simulation, *J. Atmos. Sci.*, *63*, 2437–2461.

Wang, M., et al. (2011), The multi-scale aerosol-climate model PNNL-MMF: Model description and evaluation, *Geosci. Model Dev.*, *4*(1), 137–168.

Wheeler, M. C., and H. H. Hendon (2004), An all-season real-time multivariate MJO index: Development of an index for monitoring and prediction, *Mon. Weather Rev.*, *132*, 1917–1932.

Zhang, T., P. W. Stackhouse Jr., S. K. Gupta, S. J. Cox, J. C. Mikovitz, and L. M. Hinkelman (2013), The validation of the GEWEX SRB surface shortwave flux data products using BSRN measurements: A systematic quality control, production and application approach, *J. Quant. Spectrosc. Radiat. Transfer*, *122*, 127–140, doi:10.1016/j.jqsrt.2012.10.004.